Genomic Bayesian confirmatory factor analysis and Bayesian network to characterize a wide spectrum of rice phenotypes

Haipeng Yu[1], Malachy Campbell[2], Qi Zhang[3], Harkamal Walia[2], and Gota Morota[1]

[1]Department of Animal and Poultry Sciences, Virginia Polytechnic Institute and State University, Blacksburg, VA 24061
[2]Department of Agronomy and Horticulture, University of Nebraska-Lincoln, Lincoln, NE 68583
[3]Department of Statistics, University of Nebraska-Lincoln, Lincoln, NE 68583

2

Keywords: Bayesian network, factor analysis, multi-phenotypes, rice

Running title: Network analysis in rice

Corresponding author:

Gota Morota

Department of Animal and Poultry Sciences

Virginia Polytechnic Institute and State University

Blacksburg, VA 24061, USA.

E-mail: morota@vt.edu

Abstract

Drawing biological inferences from large data generated to dissect the genetic basis of complex traits remains a challenge. Since multiple phenotypes likely share mutual relationships, elucidating the interdependencies among economically important traits can accelerate the genetic improvement of plants and animals. A Bayesian network depicts a probabilistic directed acyclic graph representing conditional dependencies among variables. This study aims to characterize various phenotypes in rice (*Oryza sativa*) via confirmatory factor analysis and Bayesian network. Confirmatory factor analysis under the Bayesian treatment hypothesized that 48 observed phenotypes resulted from six latent variables including grain morphology, morphology, flowering time, physiology (e.g., ion content), yield, and morphological salt response. This was followed by studying the genetics of each latent variable. Bayesian network structures involving the genomic component of six latent variables were established by fitting four different algorithms. Negative genomic correlations were obtained between salt response and yield, salt response and grain morphology, salt response and physiology, and morphology and yield, whereas a positive correlation was obtained between yield and grain morphology. There were four common directed edges across the different Bayesian networks. Physiological components influenced the flowering time and grain morphology, and morphology and grain morphology influenced yield. This work suggests that the Bayesian network coupled with factor analysis can provide an effective approach to understand the interdependence patterns among phenotypes and to predict the potential influence of external interventions or selection related to target traits in the high-dimensional interrelated complex traits systems.

Introduction

Genetic correlation constitutes a major aspect of quantitative genetics (Lush, 1948; Falconer and Mackay, 1996). In its simplest form, a single gene or mutation may affect several biological pathways leading to correlated phenotypes. This phenomenon, known as pleiotropy, induces genetic correlations among multiple traits at the population level. In plant and animal breeding, more than one phenotype is generally assessed to account for the overall performance of individuals. Because multiple phenotypes may exhibit mutual relationships, knowledge of the interdependence among economically important traits can bring more effective selection and genetic improvement in systems with complex traits. In a standard quantitative genetic analysis, multivariate phenotypes can be modeled through multi-trait models (MTM) of Henderson and Quaas (1976) or some genomic counterparts (e.g., Calus and Veerkamp, 2011; Jia and Jannink, 2012) by leveraging genetic or environmental correlations among traits. In particular, MTM has been useful in deriving genetic correlations and enhancing the prediction accuracy of breeding values for traits with low heritablity via joint modeling with one or more genetically correlated, highly heritable traits (Mrode, 2014). However, genetic selection for breeding requires causal assumptions, as the effects of external interventions on interrelated complex traits cannot be predicted on the basis of these associations (Pearl, 2009). This modeling step is essential to verify that predictors considered for selection accurately reflect genetic causal effects (Valente et al., 2015). Although Bayesian network (BN) analysis or causal structure inference from observational data has been an active research area in plant and animal breeding (Valente et al., 2010; Töpner et al., 2017), the primary challenge associated with multivariate analysis is that computation can be untenable. This is because the number of estimated parameters within the model increases with the increasing number of phenotypes and the difficulty of interpreting interrelationships among multiple phenotypes. This is a particularly persistent challenge in plant breeding, owing to the availability of high-dimensional and diverse phenotypes currently being gener-

4

⁷⁰ ated via high-throughput, image-based phenomics platforms in addition to the conventional,

⁷¹ non-image phenotypes (Awada et al., 2018).

⁷² One approach to characterize high-dimensional phenotypes is by using factor analysis,

⁷³ which facilitates modeling correlated responses through underlying unobserved latent vari-

⁷⁴ ables, which are also known as factors or modules (de los Campos and Gianola, 2007).

⁷⁵ Confirmatory factor analysis, a variant of factor analysis, hypothesizes that observed pheno-

⁷⁶ types result from lower-dimensional latent variables specified by prior biological knowledge

⁷⁷ (Jöreskog, 1969). These latent variables underlie observed phenotypes and can be evalu-

⁷⁸ ated for how well the data support the hypothesis. For instance, Peñagaricano et al. (2015)

⁷⁹ performed confirmatory factor analysis in swine to derive five latent variables from 19 pheno-

⁸⁰ typic traits and inferred BN structures among those latent variables, thereby demonstrating

⁸¹ the potential of this approach.

⁸² This study aimed to obtain a first glimpse of the utility of graphical modeling to char-

⁸³ acterize a wide range of phenotypes in rice by studying the genetics of each latent variable.

⁸⁴ First, we constructed latent variables, using prior biological knowledge obtained from the

⁸⁵ literature. Then we connected the observed high-dimensional phenotypes with these to

⁸⁶ establish latent variables via Bayesian confirmatory factor analysis (BCFA) to reduce the

⁸⁷ dimensions of the dataset. Further, factor scores computed from BCFA were considered

⁸⁸ new phenotypes for a Bayesian multivariate analysis to separate breeding values from noise.

⁸⁹ This was followed by adjustment of breeding values via Cholesky decomposition to eliminate

⁹⁰ the dependencies introduced by genomic relationships. Finally, the adjusted breeding values

⁹¹ were considered inputs to assess the causal network structure between latent variables by

⁹² conducting a Gaussian BN analysis. This study is the first, to our knowledge, in rice to

⁹³ characterize various phenotypes with graphical modeling such as BCFA and BN.

Materials and Methods

Sources of phenotypic and genotypic data

The rice dataset comprised $n = 413$ accessions sampled from six subpopulations: temperate japonica (92), tropical japonica (85), indica (77), aus (52), aromatic (12), and admixture of japonica and indica (56). We used $t = 48$ phenotypes and data regarding 44,000 single-nucleotide polymorphisms (SNP). Of those, 34 phenotypic records were reported in Zhao et al. (2011). The remaining phenotypes were assessed from the abiotic stress experiments conducted in Campbell et al. (2017a). The detailed descriptions of the phenotypes used can be found in Zhao et al. (2011) and Campbell et al. (2017a), and are summarized in Supplementary Table S1. After removing SNP markers with minor allele frequency less than 0.05, 374 accessions and 33,584 markers were used for further analysis.

Bayesian confirmatory factor analysis

A confirmatory factor analysis under the Bayesian framework was performed to model 48 phenotypes. The number of factors and the pattern of phenotype-factor relationships need to be specified in BCFA prior to model fitting. We constructed six latent variables ($q = 6$) from previous reports (Acquaah, 2009; Zhao et al., 2011; Campbell et al., 2017a). The six latent variables derived from our analysis represent the grain morphology, morphology, flowering time, physiology, yield, and salt response (Table S1). Each latent variable captures common signals spanning genetic and environmental effects across all its phenotypes. The latent variables, which determine the observed phenotypes can be modeled as

$$\mathbf{T} = \mathbf{\Lambda F} + \mathbf{s},$$

6

where $\mathbf{T}$ is the $t \times n$ matrix of observed phenotypes, $\mathbf{\Lambda}$ is the $t \times q$ factor loading matrix, $\mathbf{F}$ is the $q \times n$ latent variables matrix, and $\mathbf{s}$ is the $t \times n$ matrix of specific effects. Here, $\mathbf{\Lambda}$ maps latent variables to the observed variables and can be interpreted as the extent of contribution each latent variable to phenotype. This can be derived by solving the following variance-covariance model.

$$var(\mathbf{T}) = \mathbf{\Lambda}\mathbf{\Phi}\mathbf{\Lambda}' + \mathbf{\Psi},$$

where $\mathbf{\Phi}$ is the variance of latent variables, and $\mathbf{\Psi}$ is the variance of specific effects (Brown, 2014). Six latent variables were assumed to account for the covariance in the observed phenotypes. Moreover, latent variables were assumed to be correlated with each other. Prior distributions were assigned to all unknown parameters. The non-zero coefficient within factor loading matrix $\mathbf{\Lambda}$ was assumed to follow a Gaussian distribution with mean of 0 and variance of 0.01. The variance-covariance matrix $\mathbf{\Phi}$ was assigned an inverse Wishart distribution with a 6×6 identity scale matrix $\mathbf{I}_{66}$ and a degree freedom of 7, $\mathbf{\Phi} \sim \mathcal{W}^{-1}(\mathbf{I}_{66}, 7)$ and an inverse Gamma distribution with scale parameter 1 and shape parameter 0.5 was assigned to $\mathbf{\Psi} \sim \Gamma^{-1}(1, 0.5)$.

We employed the blavaan R package (Merkle and Rosseel, 2018) jointly with JAGS (Hornik et al., 2003) to fit the above BCFA. The blavaan runs the runjags R package (Denwood, 2016) to summarize the Markov chain Monte Carlo (MCMC) and samples unknown parameters from the posterior distributions. Three MCMC chains, each of 5,000 samples with 2,000 burn-in, were used to infer the unknown model parameters. The convergence of the parameters was investigated with trace plots and potential scale reduction factor (PSRF; Gelman and Rubin, 1992). The PSRF computes the difference between estimated variances among multiple Markov chains and estimated variances within the chain. A large difference indicates non-convergence and may require additional Gibbs sampling.

Subsequently, the posterior means of factor scores ($\mathbf{F}$), which reflect the contribution of

7

125 latent variables to each accession were estimated. Within each draw of Gibbs sampling, $\mathbf{F}$

126 was sampled from the conditional distribution of $p(\mathbf{F}|\boldsymbol{\theta}, \mathbf{T})$, where $\boldsymbol{\theta}$ refers to the unknown

127 parameters in $\boldsymbol{\Lambda}$, $\boldsymbol{\Phi}$, and $\boldsymbol{\Psi}$. This conditional distribution was derived with data augmenta-

128 tion (Tanner and Wong, 1987) assuming $\mathbf{F}$ as missing data (Lee and Song, 2012).

129 Multivariate genomic best linear unbiased prediction

We fitted a Bayesian multivariate genomic best linear unbiased prediction to separate breeding values from population structure and noise in the six factor scores computed previously.

$$\mathbf{F} = \boldsymbol{\mu} + \mathbf{Xb} + \mathbf{Zu} + \boldsymbol{\epsilon},$$

130 where $\boldsymbol{\mu}$ is the vector of intercept, $\mathbf{X}$ is the incidence matrix of covariates, $\mathbf{b}$ is the vector of

131 covariate effects, $\mathbf{Z}$ is the incidence matrix relating accessions with additive genetic effects, $\mathbf{u}$

132 is the vector of additive genetic effects, and $\boldsymbol{\epsilon}$ is the vector of residuals. The incident matrix

133 $\mathbf{X}$ included subpopulation information (temperate japonica, tropical japonica, indica, aus,

134 aromatic, and admixture), as the rice diversity panel used herein shows a clear substructure

135 (Zhao et al., 2011).

A flat prior was assigned to $\boldsymbol{\mu}$ and $\mathbf{b}$, and the joint distribution of $\mathbf{u}$ and $\boldsymbol{\epsilon}$ follows multivariate normal

$$\begin{pmatrix} \mathbf{u} \\ \boldsymbol{\epsilon} \end{pmatrix} \sim N \left[\begin{pmatrix} \mathbf{0} \\ \mathbf{0} \end{pmatrix}, \begin{pmatrix} \boldsymbol{\Sigma_u} \otimes \mathbf{G} & \mathbf{0} \\ \mathbf{0} & \boldsymbol{\Sigma_\epsilon} \otimes \mathbf{I} \end{pmatrix} \right],$$

136 where $\mathbf{G}$ represents the second genomic relationship matrix of VanRaden (2008), $\mathbf{I}$ is the

137 identity matrix, $\boldsymbol{\Sigma_u}$ and $\boldsymbol{\Sigma_\epsilon}$ refer to 6×6 dimensional genetic and residual variance-covariance

138 matrices, respectively. An inverse Wishart distribution with a 6×6 identity scale matrix of $\mathbf{I}_{66}$

139 and a degree of freedom 6 was assigned as prior for $\boldsymbol{\Sigma_u}, \boldsymbol{\Sigma_e} \sim \mathcal{W}^{-1}(\mathbf{I}_{66}, 6)$. These parameters

140 were selected so that relatively uninformative priors were used. The Bayesian multivariate

8

141 genomic best linear unbiased prediction model was implemented using the MTM R pack-

142 age (https://github.com/QuantGen/MTM). Posterior mean estimates of genetic correlation

143 between latent variables and predicted breeding values ($\hat{\mathbf{u}}$) were then obtained.

Sample independence in the Bayesian network

Theoretically, BN learning algorithms assume sample independence. In the multivariate genomic best linear unbiased prediction, the residuals between phenotypes were assumed independent through $\mathbf{I_{374x374}}$. However, phenotypic dependencies were introduced by the $\mathbf{G}$ matrix for the additive genetic effects, thereby potentially serving as a confounder. Thus, a transformation of $\hat{\mathbf{u}}$ was carried out to derive an adjusted $\hat{\mathbf{u}}^*$ by eliminating the dependencies in $\mathbf{G}$. For a single trait model, the adjusted $\hat{\mathbf{u}}^*$ can be computed by premultiplying $\hat{\mathbf{u}}$ by $\mathbf{L}^{-1}$, where $\mathbf{L}$ is a lower triangular matrix derived from the Choleskey decompostion of $\mathbf{G}$ matrix ($\mathbf{G} = \mathbf{LL}'$). Since $\mathbf{u} \sim \mathcal{N}(0, \mathbf{G}\sigma_u^2)$, the distribution of $\hat{\mathbf{u}}^*$ follows $\mathcal{N}(0, \mathbf{I}\sigma_u^2)$ (Vazquez et al., 2010)

$$
\begin{aligned}
Var(\mathbf{u}^*) &= Var(\mathbf{L^{-1}u}) \\
&= \mathbf{L^{-1}}Var(\mathbf{u})(\mathbf{L^{-1}})^{'} \\
&= \mathbf{L^{-1}}\mathbf{G}(\mathbf{L^{-1}})^{'}\sigma_u^2 \\
&= \mathbf{L^{-1}}\mathbf{LL}^{'}(\mathbf{L}')^{-1}\sigma_u^2 \\
&= \mathbf{I}\sigma_u^2.
\end{aligned}
$$

145 This transformation can be extended to a multi-traits model by defining $\mathbf{u}^* = \mathbf{M^{-1}u}$, where

146 $\mathbf{M^{-1}} = \mathbf{I_{qq}} \otimes \mathbf{L^{-1}}$ (Töpner et al., 2017). Under the multivariate framework, $\mathbf{u}$ follows

147 $\mathcal{N}(0, \mathbf{\Sigma_u} \otimes \mathbf{G})$ and the variance of $\mathbf{u}^*$ is

$$Var(\mathbf{u}^*) = Var(\mathbf{M^{-1}u})$$

$$= (\mathbf{I_{tt}} \otimes \mathbf{L^{-1}})(\mathbf{\Sigma_u} \otimes \mathbf{G})(\mathbf{I_{qq}} \otimes \mathbf{L^{-1}})'$$

$$= (\mathbf{I_{qq}} \otimes \mathbf{L^{-1}})(\mathbf{\Sigma_u} \otimes \mathbf{LL'})(\mathbf{I_{qq}} \otimes \mathbf{L^{-1}})'$$

$$= \mathbf{\Sigma_u} \otimes \mathbf{I_{nn}},$$

where $\mathbf{L^{-1}LL'(L^{-1})'} = \mathbf{I_{nn}}$. This adjusted $\mathbf{\hat{u}}^*$ was used to learn BN structures between predicted breeding values.

Bayesian network

A BN depicts the joint distribution of random variables regarding their probabilistic conditional dependencies (Scutari and Denis, 2014)

$$\mathcal{BN} = (\mathcal{G}, X_V),$$

where $\mathcal{G}$ represents a directed acyclic graph (DAG) $= (V, E)$ with nodes (V) connected by one or more edges (E) conveying the probabilistic relationships and the random vector $X_V = (X_1, ..., X_K)$ is K random variables. The joint probability distribution can be factorized as

$$P(X_V) = P(X_1, ..., X_K) = \prod_{v=1}^{K} P(X_v|Pa(X_v)),$$

where $Pa(X_v)$ denotes a set of parent nodes of child node X_v. The DAG and joint probability distribution are governed by the Markov condition, which states that every random variable is independent of its non-descendants conditioned on its parents. A BN is known as a Gaussian BN, when all variables or phenotypes are defined as marginal or conditional Gaussian distribution as in the present study.

156 The adjusted breeding values $\hat{\mathbf{u}}^*$ were used to infer a genomic network structure among

157 the aforementioned six latent variables. There are three types of structure-learning algo-

158 rithms for BN: constraint-based algorithms, score-based algorithms, and a hybrid of these

159 two (Scutari and Denis, 2014). The constraint-based algorithms can be originally traced

160 to the inductive causation algorithm (Verma and Pearl, 1991), which uses conditional in-

161 dependence tests for network inference. Briefly, the first step is to identify a d-separation

162 set for each pair of nodes and confer an undirected edge between the two if they are not

163 d-separated. The second step is to identify a v-structure for each pair of non-adjacent nodes,

164 where a common neighbor is the outcome of two non-adjacent nodes. In the last step, com-

165 pelled edges were identified and oriented, where neither cyclic graph nor new v-structures

166 are permitted. The score-based algorithms are based on heuristic approaches, which first

167 assign a goodness-of-fit score for an initial graph structure and then maximize this score by

168 updating the structure (i.e., add, delete, or reverse the edges of initial graph). The hybrid

169 algorithm includes two steps, restrict and maximize, which harness both constrain-based and

170 score-based algorithms to construct a reliable network. In this study, the two score-based

171 (Hill Climbing and Tabu) and two hybrid algorithms (Max-Min Hill Climbing and General

172 2-Phase Restricted Maximization) were used to perform structure learning.

173 We quantified the strength of edges and uncertainty regarding the direction of networks,

174 using 500 bootstrapping replicates with a size equal to the number of accessions and per-

175 formed structure learning for each replicate in accordance with Scutari and Denis (2014).

176 Non-parametric bootstrap resampling aimed at reducing the impact of the local optimal

177 structures by computing the probability of the arcs and directions. Subsequently, 500 learned

178 structures were averaged with a strength threshold of 85% or higher to produce a more robust

179 network structure. This process, known as model averaging, returns the final network with

180 arcs present in at least 85% among all 500 networks. Candidate networks were compared

181 on the basis of the Bayesian information criterion (BIC) and Bayesian Gaussian equivalent

182 score (BGe). The BIC accounts for the goodness-of-fit and model complexity, and BGe aims

11

183 at maximizing the posterior probability of networks per the data. All BN were learned via

184 the bnlearn R package (Scutari, 2010). In bnlearn, the BIC score is rescaled by -2, which

185 indicates that the larger BIC refers to a preferred model.

Data availability

187 Genotypic data regarding the rice accessions can be downloaded from the rice diversity panel

188 website (`http://www.ricediversity.org/`). Phenotypic data used herein are available in

189 Zhao et al. (2011) and Campbell et al. (2017b).

Results

Latent variable modeling

The BCFA model grouped the observed phenotypes into the underlying latent variables on the basis of prior biological knowledge, assuming these latent variables determine the observed phenotypes. This allowed us to study the genetics of each latent variable. A measurement model derived from BCFA evaluating the six latent variables is shown in Figure 1. Forty-eight observed phenotypes were hypothesized to result from the six latent variables: 7 for flowering time, 14 for morphology, 5 for yield, 11 for grain morphology, 6 for physiology, and 5 for salt response. The convergence of the parameters was confirmed graphically with the trace plots and a PSRF value less than 1.2 (Merkle and Rosseel, 2018).

The six latent factors showed strong contributions to the 48 observed phenotypes, with standardized regression coefficients ranging from -0.668 to 0.980 for flowering time, -0.112 to 0.903 for morphology, -0.113 to 0.977 for yield, -0.501 to 0.986 for grain morphology, -0.016 to 0.829 for physiology, and 0.011 to 0.929 for salt response. The latent factor flowering time showed a strong positive contribution to flowering time in Arkansas (Fla) and Flowering time in Arkansas in 2007 (Fla7), indicating that larger values for the latent factor can be interpreted as a greater number of days from sowing to emergence of the inflorescence. The latent factor morphology showed the largest positive contributions to traits describing height during the vegetative stage (e.g. height to newest ligule in salt (Hls), height to newest ligule in control (Hlc), height to the tip of first fully expanded leaf in salt (Hfs), and height to tip of first fully expanded leaf in control (Hfc)), suggesting that this latent factor is an overall representation of plant size. Yield showed large positive contributions to the observed phenotypes primary panicle branch number (Ppn) and seed number per panicle (Snpp), suggesting that larger values for yield indicate a higher degree of branching and seed number. Observed phenotypes describing seed size (e.g. seed volume (Sv) and brown rice

13

215 volume (Bvl)) were most strongly associated with grain morphology. The latent factor ionic

216 components of salt stress showed strong positive contributions to two observed phenotypes

217 that quantify the ionic components of salt stress (shoot Na^+:K^+ (Kslm) and shoot Na^+

218 (Nas)), indicating that higher values for the latent factor result in greater shoot Na^+ and

219 Na^+:K^+. Finally, the latent factor describing morphological salt response showed strong

220 positive contributions to the observed phenotype describing the effect of salt treatment on

221 plant height (ratio of height to tip of newest fully expanded leaf in salt to that of control

222 plants (Hfr)), thus larger values for the latent factor may indicate a more tolerant growth

223 response to salinity.

Genomic correlation among latent variables

225 To understand the genetic relationships between latent variables, genomic correlation analy-

226 sis was performed. Genomic correlation is due to pleiotropy or linkage disequilibrium between

227 quantitative trait locus (QTL). The genomic correlations among latent variables are shown

228 in Figure 2. Negative correlations were observed between salt response (Slr) and all other

229 five latent variables. In particular, flowering time (-0.5), yield (-0.54), and grain morphology

230 (-0.74) were moderately correlated with morphological salt response. These results suggest

231 that accessions that harbor alleles for more tolerant morphological salt responses may also

232 have alleles associated with longer flowering times, smaller seeds, and low yield. Similarly,

233 a moderate negative correlation was observed between morphology and yield (-0.56) and

234 between morphology and grain morphology (-0.31). Thus, accessions with alleles associated

235 with large plant size may also have alleles that result in low yield, small grain volume, and

236 lower shoot Na^+ and Na^+:K^+. In contrast, a positive moderate correlation was observed

237 between grain morphology and yield (0.49) and between grain morphology and ionic com-

238 ponents of salt stress (0.4). Thus, selection for large grain may result in improved yield, and

239 higher shoot Na^+ and Na^+:K^+.

14

Bayesian network

To infer the possible causal structure between latent variables, BN was performed. Prior to BN, the normality of latent variables was assessed using histogram plots combined with density curves as shown in Figure S1. Overall, all the six latent variables approximately followed a Gaussian distribution.

The Bayesian networks learned with the score-based and hybrid algorithms are shown in Figures 3, 4, 5, and 6. The structures of BN were refined by model averaging with 500 networks from bootstrap resampling to reduce the impact of local optimal structures. The labels of the arcs measure the uncertainty of the arcs, corresponding to strength and direction (in parenthesis). The former measures the frequency of the arc presented among all 500 networks from the bootstrapping replicates and the latter is the frequency of the direction shown conditional on the presence of the arc. We observed minor differences in the structures presented within and across the two types of algorithms used. In general, small differences were observed within algorithm types compared to those across algorithms. The two score-based algorithms produced a greater number of edges than two hybrid algorithms. In Figure 3, the Hill Climbing algorithm produced seven directed connections among the six latent variables. Three connections were indicated towards flowering time from morphological salt response, ionic components of salt stress, and morphology, and two edges to yield from morphology and from grain morphology. Other two edges were observed from ionic components of salt stress to grain morphology and from grain morphology to morphological salt response. A similar structure was generated by the Tabu algorithm, except that the connection between salt response and grain morphology presented an opposite direction (Figure 4). The Max-Min Hill Climbing hybrid algorithm yielded six directed edges from morphological salt response to grain morphology, from ionic components of salt stress to grain morphology, from ionic components of salt stress to flowering time, from flowering time to morphology, from morphology to yield, and from grain morphology to yield (Figure 5). An analogous structure

15

266 with the only difference observed in the directed edge from morphology to flowering time was

267 inferred with the General 2-Phase Restricted Maximization algorithm as shown in Figure 6.

268 Across all four algorithms, there were four common directed edges: from ionic components

269 of salt stress to flowering time and to grain morphology, and from morphology and grain

270 morphology to yield. The most favorable network was considered the one from the Tabu

271 algorithm, which returned the largest network score in terms of BIC (1086.61) and BGe

272 (1080.88). Collectively, these results suggest that there may be a direct genetic influence of

273 morphology and grain morphology on yield, and physiological components of salt tolerance

274 on grain morphology and flowering time.

Discussion

This study is based on the premise that most phenotypes interact to greater or lesser degrees with each other through underlying physiological and molecular pathways. While these physiological pathways are important for the development of agronomically important characteristics, they are often unknown or difficult to assess in large populations. The approach utilized here leverages phenotypes that can be readily assessed in large populations to quantify these underlying unobserved phenotypes, and elucidates the relationships between these variables.

Understanding the behaviors among phenotypes in the complex traits is critical for genetic improvement of agricultural species (Hickey et al., 2017). Graphical modeling offers an avenue to decipher bi-directional associations or probabilistic dependencies among variables of interest in plant and animal breeding. For instance, BN and L1-regularized undirected network can be used to model interrelationships of linkage disequilibrium (LD) (Morota et al., 2012; Morota and Gianola, 2013) or phenotypic, genetic, and environmental interactions (Xavier et al., 2017) in a systematic manner. Importantly, MTM elucidates both direct and indirect relationships among phenotypes. Inaccurate interpretation of these relationships may substantially bias selection decisions (Valente et al., 2015; Gianola et al., 2015). Thus, we applied BCFA to reduce the dimension of the responses by hypothesizing 48 manifest phenotypes originated from the underlying six constructed latent variables as shown in Figure 1 assuming that these latent traits are most important, followed by application of BN to infer the structures among the six biologically relevant latent variables (Figures 3,4, 5, and 6). The BN represents the conditional dependencies between variables. Care must be taken in interpreting these relationships as a causal effect. Although a good BN is expected to describe the underlying causal structure per the data, when the structure is learned solely on the basis of the observed data, it may return multiple equivalent networks that describe the data well. In practice, searching such a causal structure with observed data needs three

17

additional assumptions (Scutari and Denis, 2014): 1) each variable is independent of its non-effects (i.e., direct and indirect) conditioned on its direct causes, 2) the probability distribution of variables is supported by a DAG, where the d-separation in DAG provides all dependencies in the probability distribution, and 3) no additional variables influence the variables within the network. Although it may be difficult to meet these assumptions in the observed data, a BN is equipped with suggesting potential causal relationships among latent variables, which can assist in exploring data, making breeding decisions, and improving management strategies in breeding programs (Rosa et al., 2011).

Biological meaning of latent variables and their relationships

We performed BCFA to summarize the original 48 phenotypes with the six latent variables. The number of latent variables and which latent variables load onto phenotypes were determined from the literature. The latent variable morphological salt response (Slr) contributed strongly to salt indices for shoot biomass, root biomass, and two indices for plant height. Thus, morphological salt response can be interpreted as the morphological responses to salinity stress, with higher values indicating a more tolerant growth response. The latent variable yield is a representation of overall grain productivity, and contributed strongly to the observed phenotypes primary panicle branch number, seed number per panicle, and panicle length. The positive loading scores on these observable phenotypes indicates that more highly branched, productive panicles will have higher values for yield. Seed width, seed volume, and seed surface area contributed significantly to the latent variable grain morphology (Grm). Therefore, these results indicate that the grain morphology is a summary of the overall shape of the grain, where high values represent large, round grains, while low values represent small, slender grains. Considering the grain characteristics of rice subpopulations, temperate japonica accessions are expected to have high values for grain morphology, while

18

326 indica accessions have lower values for grain morphology. Latent variable morphology (Mrp)
327 is a representation of plant biomass during the vegetative stage (28-day-old plants). Shoot
328 biomass, root biomass, and two metrics for plant height contributed largely to morphol-
329 ogy, suggesting that accessions with high values for morphology are tall plants with a large
330 biomass.

331 Genomic correlation analysis among the six latent variables showed moderate correlations
332 among several pairs. These genetic correlations can either be caused by linkage or pleitropy.
333 The former is likely to prevail in species with high LD, which is the case in rice where
334 LD ranges from 100 to 200kb (Huang et al., 2010). A strong negative relationship was
335 observed between morphological salt response and three other latent variables. For instance,
336 a negative correlation between morphological salt response and yield indicates that accessions
337 of samples harboring alleles for superior morphological salt responses (e.g. those that are
338 more tolerant) tend to also harbor alleles for poor yield. The rice diversity panel we used
339 is a representative sample of the total genetic diversity within cultivated rice and contains
340 many unimproved traditional varieties and modern breeding lines (Eizenga et al., 2014).
341 While traditional varieties exhibit superior adaptation to abiotic stresses, they often have
342 very poor agronomic characteristics including low yield, late flowering, and high photoperiod
343 sensitivity (Thomson et al., 2009, 2010). Moreover, the indica and japonica subspecies have
344 contrasting salt responses and very different grain morphology. Japonica accessions tend to
345 have short, round seeds and are more sensitive to salt stress, while indica accessions have
346 long, slender grains and often are more salt tolerant (Zhao et al., 2011; Campbell et al.,
347 2017a). The negative relationship observed between salt response and grain morphology
348 suggests that lines that harbor alleles for high grain morphology (e.g., large, round grains)
349 tend to also harbor alleles for a tolerant growth response to salt stress. However, no studies
350 have yet reported an association between alleles for grain morphology and morphological
351 salt response. Therefore, it remains to be addressed whether this relationship is due to LD
352 or pleitropy.

19

353 Genetic correlations observed between other latent variables may suggest a pleiotropic
354 effect among loci. For instance, a moderate negative relationship was observed between
355 morphological salt response and ionic components of salt stress, indicating that accessions
356 harboring alleles associated with superior morphological salt response also tend to harbor
357 alleles for reduced ion content under salt stress. The relationship between salt tolerance,
358 measured in terms of growth or yield, and Na^+ and Na^+:K^+ has been a documented for
359 decades (reviewed by Munns and Tester (2008)). Moreover, natural variation for Na^+ trans-
360 porters has been utilized to improve growth and yield under saline conditions in rice and
361 other cereals (Ren et al., 2005; Byrt et al., 2007; Horie et al., 2009; Munns et al., 2012;
362 Campbell et al., 2017a). Therefore, the negative genetic relationships observed between
363 morphological salt response and ion content may be due to the pleiotropic effects of some
364 loci.

365 The genomic relationships among latent variables including morphology, yield, and grain
366 morphology may have resulted from the selection of alleles associated with good agronomic
367 characteristics. A moderate positive relationship was observed between yield and grain mor-
368 phology, suggesting that alleles that positively contribute to productive panicles also may
369 contribute to large, round grains. Furthermore, the negative genomic correlation observed be-
370 tween morphology and yield indicates that alleles negatively influencing total plant biomass
371 also have a positive contribution to traits for productive panicles. This genomic relationship
372 may reflect the genetics of harvest index, which is defined as the ratio of grain yield to total
373 biomass. Over the past 50 years, rice breeders have selected high harvest index, resulting
374 in plants with short compact morphology and many highly productive panicles (Hay, 1995;
375 Peng et al., 2008).

376 Although BCFA may yield biologically meaningful results, a potential limitation of BCFA
377 is that we assumed each phenotype does not measure more than one latent variable. This
378 assumption may not always strictly concur with the observational data. Therefore, further
379 studies are required to allow each phenotype to potentially load onto multiple factors in the

20

380 BCFA framework. An alternative approach is to derive the number of latent variables and
381 determine which latent variables load onto phenotypes directly from observed data, using
382 exploratory factor analysis. This approach was not pursued here because accurate estimation
383 of unknown parameters in the exploratory factor analysis requires a large sample size, which
384 was not the case herein (Brown, 2014).

Bayesian network of latent variables

386 The BN is a probabilistic DAG, which represents the conditional dependencies among phe-
387 notypes. The genomic correlation among latent variables described in Figure 2 does not
388 inform the flow of genetic signals nor distinguish direct and indirect associations, whereas
389 BN displays directions between latent variables and separate direct and indirect associations.
390 Therefore, the BN describes the possibility that other phenotypes will change if one pheno-
391 type is intervened (i.e., selection). However, caution is required to interpret this network as
392 a causal effect, as the causal BN requires more assumptions, which are usually difficult to
393 meet in observational data (Pearl, 2009).

394   Four common edges or consensus subnetworks across the four BN may be the most
395 reliable substructure of latent variables and may describe the dependence between agronomic
396 traits (Figures 3, 4, 5, and 6). For example, edges from grain morphology to yield and
397 morphology to yield can be interpreted as final grain productivity is dependant on specific
398 vegetative characteristics as well grain traits. This is because yield, which represents the
399 overall grain productivity of a plant, depends on morphological characteristics such as the
400 degree of tillering, an architecture that allows the plant to efficiently capture light and
401 carbon, and a stature that is resistant to lodging, the degree of panicle branching, as well
402 as specific grain characteristics such as seed volume and shape. Moreover, there is a direct
403 biological linkage between specific vegetative architectural traits such as tillering and plant
404 height, and yield related traits such as panicle branching and number of seeds per panicle.
405 The degree of branching during both vegetative and reproductive development is dependant

21

on the development and initiation of auxiliary meristems. Several genes have been identified in this pathway and have shown to have pleiotropic effects on tillering and panicle branching (reviewed by Liang et al. (2014)). For instance, *OsSPL14* has been shown to be an important regulator of auxiliary branching in both vegetative and reproductive stages in rice (Jiao et al., 2010; Miura et al., 2010). Moreover, other genes such as *OsGhd8* have been reported to regulate other morphological traits such as plant height and yield through increase panicle branching (Yan et al., 2011). The biological importance of these dependencies can also be illustrated by viewing them in the context of genetic improvement, as selection for specific architectural traits (represented by the latent variable morphology) and grain characteristics have traditionally been used as traits to improve rice productivity in many conventional breeding programs (Redona and Mackill, 1998; Huang et al., 2013).

While the above example provides a plausible network structure between latent variables, edges from ionic components of salt stress to flowering time and to grain morphology are an example of instances where caution should be used to infer causation. As mentioned above, there is an inherent difference in salt tolerance and grain morphological traits between the indica and japonica subspecies. The edges observed for these two latent variables (ionic components of salt stress and grain morphology) in BN may be driven by LD between alleles associated with grain morphology and alleles for salt tolerance rather than pleitropy. Thus, given the current data set, genetic effects for grain morphology may still be conditionally dependant on ionic components of salt stress and the BN may be true, even if there is no direct overlap in the genetic mechanisms for the two traits.

We found that there are some uncertain edges among BN. For instance, direction from salt response to grain morphology is supported by 65% (Figure 4), 58% (Figure 5), and 58% (Figure 6) bootstrap sampling, whereas the opposite direction is supported by 56% bootstrap sampling (Figure 3). An analogous uncertainty was also observed between morphology and flowering time, i.e., the path from morphology to flowering time was supported 60% (Figure 3), 51% (Figure 4), and 52% (Figure 6), while the reverse direction was supported 51%

⁴³³ (Figure 6) upon bootstrapping. In addition, the two score-based algorithms captured edges

⁴³⁴ between morphological salt response and flowering time with 70% and 76% bootstrapping

⁴³⁵ evidence. However, this connection was not detected in the two hybrid algorithms. In

⁴³⁶ general, inferring the direction of edges was harder than inferring the presence or absence of

⁴³⁷ undirected edges. Finally, the whole structures of BN were evaluated in terms of the BIC

⁴³⁸ score and BGe. Ranking of the networks was consistent across BIC and BGe and the two

⁴³⁹ score-based algorithms produced networks with greater goodness-of-fit than the two hybrid

⁴⁴⁰ algorithms. The optimal network was produced by the Tabu algorithm. This is consistent

⁴⁴¹ with the previous study reporting that the score-based algorithm produced a better fit of

⁴⁴² networks in data on maize (Töpner et al., 2017).

⁴⁴³ In conclusion, the present results show the utility of factor analysis and network analysis

⁴⁴⁴ to characterize various phenotypes in rice. We showed that the joint use of BCFA and

⁴⁴⁵ BN can be applied to predict the potential influence of external interventions or selection

⁴⁴⁶ associated with target traits such as yield in the high-dimensional interrelated complex traits

⁴⁴⁷ system. We contend that the approaches used herein provide greater insights than pairwise-

⁴⁴⁸ association measures of multiple phenotypes and can be used to analyze the massive amount

⁴⁴⁹ of diverse image-based phenomics dataset being generated by the automated plant phenomics

⁴⁵⁰ platforms (e.g., Furbank and Tester, 2011). With a large volume of complex traits being

⁴⁵¹ collected through phenomics, numerous opportunities to forge new research directions are

⁴⁵² generated by using network analysis for the growing number of phenotypes.

References

Acquaah, G. (2009). *Principles of plant genetics and breeding.* John Wiley & Sons.

Awada, L., Phillips, P. W., and Smyth, S. J. (2018). The adoption of automated phenotyping by plant breeders. *Euphytica*, 214(8):148.

Brown, T. A. (2014). *Confirmatory factor analysis for applied research.* Guilford Publications.

Byrt, C. S., Platten, J. D., Spielmeyer, W., James, R. A., Lagudah, E. S., Dennis, E. S., Tester, M., and Munns, R. (2007). Hkt1; 5-like cation transporters linked to na+ exclusion loci in wheat, nax2 and kna1. *Plant Physiology*, 143(4):1918–1928.

Calus, M. P. and Veerkamp, R. F. (2011). Accuracy of multi-trait genomic selection using different methods. *Genetics Selection Evolution*, 43(1):26.

Campbell, M. T., Bandillo, N., Al Shiblawi, F. R. A., Sharma, S., Liu, K., Du, Q., Schmitz, A. J., Zhang, C., Véry, A.-A., Lorenz, A. J., et al. (2017a). Allelic variants of oshkt1; 1 underlie the divergence between indica and japonica subspecies of rice (oryza sativa) for root sodium content. *PLoS Genetics*, 13(6):e1006823.

Campbell, M. T., Du, Q., Liu, K., Brien, C. J., Berger, B., Zhang, C., and Walia, H. (2017b). A comprehensive image-based phenomic analysis reveals the complex genetic architecture of shoot growth dynamics in rice (oryza sativa). *The Plant Genome*, 10(2).

de los Campos, G. and Gianola, D. (2007). Factor analysis models for structuring covariance matrices of additive genetic effects: a bayesian implementation. *Genetics Selection Evolution*, 39(5):481.

Denwood, M. (2016). runjags: An r package providing interface utilities, model templates,

parallel computing methods and additional distributions for mcmc models in jags. *Journal of Statistical Software, Articles*, 71(9):1–25.

Eizenga, G. C., Ali, M., Bryant, R. J., Yeater, K. M., McClung, A. M., McCouch, S. R., et al. (2014). Registration of the rice diversity panel 1 for genomewide association studies. *Journal of Plant Registrations*, 8(1):109–116.

Falconer, D. and Mackay, T. (1996). *Introduction to Quantitative Genetics*. Pearson.

Furbank, R. T. and Tester, M. (2011). Phenomics-technologies to relieve the phenotyping bottleneck. *Trends Plant Sci.*, 16:635–644.

Gelman, A. and Rubin, D. B. (1992). Inference from iterative simulation using multiple sequences. *Statistical Science*, pages 457–472.

Gianola, D., de los Campos, G., Toro, M. A., Naya, H., Schön, C.-C., and Sorensen, D. (2015). Do molecular markers inform about pleiotropy? *Genetics*, pages genetics–115.

Hay, R. (1995). Harvest index: a review of its use in plant breeding and crop physiology. *Annals of applied biology*, 126(1):197–216.

Henderson, C. and Quaas, R. (1976). Multiple trait evaluation using relatives' records. *Journal of Animal Science*, 43(6):1188–1197.

Hickey, J. M., Chiurugwi, T., Mackay, I., Powell, W., Eggen, A., Kilian, A., Jones, C., Canales, C., Grattapaglia, D., Bassi, F., et al. (2017). Genomic prediction unifies animal and plant breeding programs to form platforms for biological discovery. *Nature genetics*, 49(9):1297.

Horie, T., Hauser, F., and Schroeder, J. I. (2009). Hkt transporter-mediated salinity resistance mechanisms in arabidopsis and monocot crop plants. *Trends in plant science*, 14(12):660–668.

25

498 Hornik, K., Leisch, F., and Zeileis, A. (2003). Jags: A program for analysis of bayesian
499   graphical models using gibbs sampling. In *Proceedings of DSC*, volume 2, pages 1–1.

500 Huang, R., Jiang, L., Zheng, J., Wang, T., Wang, H., Huang, Y., and Hong, Z. (2013).
501   Genetic bases of rice grain shape: so many genes, so little known. *Trends in plant science*,
502   18(4):218–226.

503 Huang, X., Sang, T., Zhao, Q., Feng, Q., Zhao, Y., Li, C., Zhu, C., Lu, T., Zhang, Z., Li, M.,
504   et al. (2010). Genome-wide association studies of 14 agronomic traits in rice landraces.
505   *Nature Genetics*, 42(11):961.

506 Jia, Y. and Jannink, J.-L. (2012). Multiple trait genomic selection methods increase genetic
507   value prediction accuracy. *Genetics*, pages genetics–112.

508 Jiao, Y., Wang, Y., Xue, D., Wang, J., Yan, M., Liu, G., Dong, G., Zeng, D., Lu, Z., Zhu,
509   X., et al. (2010). Regulation of osspl14 by osmir156 defines ideal plant architecture in rice.
510   *Nature genetics*, 42(6):541.

511 Jöreskog, K. G. (1969). A general approach to confirmatory maximum likelihood factor
512   analysis. *Psychometrika*, 34(2):183–202.

513 Lee, S.-Y. and Song, X.-Y. (2012). *Basic and advanced Bayesian structural equation model-*
514   *ing: With applications in the medical and behavioral sciences.* John Wiley & Sons.

515 Liang, W.-h., Shang, F., Lin, Q.-t., Lou, C., and Zhang, J. (2014). Tillering and panicle
516   branching genes in rice. *Gene*, 537(1):1–5.

517 Lush, J. L. (1948). The genetics of populations. Technical Report Mimeo.

518 Merkle, E. and Rosseel, Y. (2018). blavaan: Bayesian structural equation models via pa-
519   rameter expansion. *Journal of Statistical Software, Articles*, 85(4):1–30.

520 Miura, K., Ikeda, M., Matsubara, A., Song, X.-J., Ito, M., Asano, K., Matsuoka, M., Ki-
521 tano, H., and Ashikari, M. (2010). Osspl14 promotes panicle branching and higher grain
522 productivity in rice. *Nature genetics*, 42(6):545.

523 Morota, G. and Gianola, D. (2013). Evaluation of linkage disequilibrium in wheat with an l1-
524 regularized sparse markov network. *Theoretical and Applied Genetics*, 126(8):1991–2002.

525 Morota, G., Valente, B., Rosa, G., Weigel, K., and Gianola, D. (2012). An assessment
526 of linkage disequilibrium in holstein cattle using a bayesian network. *Journal of Animal*
527 *Breeding and Genetics*, 129(6):474–487.

528 Mrode, R. A. (2014). *Linear models for the prediction of animal breeding values*. Cabi.

529 Munns, R., James, R. A., Xu, B., Athman, A., Conn, S. J., Jordans, C., Byrt, C. S., Hare,
530 R. A., Tyerman, S. D., Tester, M., et al. (2012). Wheat grain yield on saline soils is
531 improved by an ancestral na+ transporter gene. *Nature biotechnology*, 30(4):360.

532 Munns, R. and Tester, M. (2008). Mechanisms of salinity tolerance. *Annu. Rev. Plant Biol.*,
533 59:651–681.

534 Pearl, J. (2009). *Causality: Models, Reasoning and Inference*. Cambridge University Press,
535 New York, NY, USA, 2nd edition.

536 Peñagaricano, F., Valente, B., Steibel, J., Bates, R., Ernst, C., Khatib, H., and Rosa,
537 G. (2015). Searching for causal networks involving latent variables in complex traits:
538 application to growth, carcass, and meat quality traits in pigs. *Journal of Animal Science*,
539 93(10):4617–4623.

540 Peng, S., Khush, G. S., Virk, P., Tang, Q., and Zou, Y. (2008). Progress in ideotype breeding
541 to increase rice yield potential. *Field Crops Research*, 108(1):32–38.

542 Redona, E. and Mackill, D. (1998). Quantitative trait locus analysis for rice panicle and
543 grain characteristics. *Theoretical and Applied Genetics*, 96(6-7):957–963.

Ren, Z.-H., Gao, J.-P., Li, L.-G., Cai, X.-L., Huang, W., Chao, D.-Y., Zhu, M.-Z., Wang, Z.-Y., Luan, S., and Lin, H.-X. (2005). A rice quantitative trait locus for salt tolerance encodes a sodium transporter. *Nature genetics*, 37(10):1141.

Rosa, G. J., Valente, B. D., de los Campos, G., Wu, X.-L., Gianola, D., and Silva, M. A. (2011). Inferring causal phenotype networks using structural equation models. *Genetics Selection Evolution*, 43(1):6.

Scutari, M. (2010). Learning bayesian networks with the bnlearn r package. *Journal of Statistical Software, Articles*, 35(3):1–22.

Scutari, M. and Denis, J.-B. (2014). *Bayesian networks: with examples in R.* Chapman and Hall/CRC.

Tanner, M. A. and Wong, W. H. (1987). The calculation of posterior distributions by data augmentation. *Journal of the American statistical Association*, 82(398):528–540.

Thomson, M. J., de Ocampo, M., Egdane, J., Rahman, M. A., Sajise, A. G., Adorada, D. L., Tumimbang-Raiz, E., Blumwald, E., Seraj, Z. I., Singh, R. K., et al. (2010). Characterizing the saltol quantitative trait locus for salinity tolerance in rice. *Rice*, 3(2-3):148–160.

Thomson, M. J., Ismail, A. M., McCouch, S. R., and Mackill, D. J. (2009). Marker assisted breeding. In *Abiotic Stress Adaptation in Plants*, pages 451–469. Springer.

Töpner, K., Rosa, G. J., Gianola, D., and Schön, C.-C. (2017). Bayesian networks illustrate genomic and residual trait connections in maize (Zea mays L.). *G3: Genes, Genomes, Genetics*, 7(8):2779–2789.

Valente, B. D., Morota, G., Peñagaricano, F., Gianola, D., Weigel, K., and Rosa, G. J. (2015). The causal meaning of genomic predictors and how it affects construction and comparison of genome-enabled selection models. *Genetics*, 200(2):483–494.

Valente, B. D., Rosa, G. J., de los Campos, G., Gianola, D., and Silva, M. A. (2010). Searching for recursive causal structures in multivariate quantitative genetics mixed models. *Genetics*, 185(2):633–644.

VanRaden, P. M. (2008). Efficient methods to compute genomic predictions. *J. Dairy Sci.*, 91:4414–4423.

Vazquez, A., Bates, D., Rosa, G., Gianola, D., and Weigel, K. (2010). An r package for fitting generalized linear mixed models in animal breeding 1. *Journal of animal science*, 88(2):497–504.

Verma, T. and Pearl, J. (1991). Equivalence and synthesis of causal models. In *Proceedings of the Sixth Annual Conference on Uncertainty in Artificial Intelligence*, UAI '90, pages 255–270, New York, NY, USA. Elsevier Science Inc.

Xavier, A., Hall, B., Casteel, S., Muir, W., and Rainey, K. M. (2017). Using unsupervised learning techniques to assess interactions among complex traits in soybeans. *Euphytica*, 213(8):200.

Yan, W.-H., Wang, P., Chen, H.-X., Zhou, H.-J., Li, Q.-P., Wang, C.-R., Ding, Z.-H., Zhang, Y.-S., Yu, S.-B., Xing, Y.-Z., et al. (2011). A major qtl, ghd8, plays pleiotropic roles in regulating grain productivity, plant height, and heading date in rice. *Molecular plant*, 4(2):319–330.

Zhao, K., Tung, C.-W., Eizenga, G. C., Wright, M. H., Ali, M. L., Price, A. H., Norton, G. J., Islam, M. R., Reynolds, A., Mezey, J., et al. (2011). Genome-wide association mapping reveals a rich genetic architecture of complex traits in oryza sativa. *Nature Communications*, 2:467.

Tables

Table 1: Standardized factor loadings obtained from the Bayesian confirmatory factor analysis.

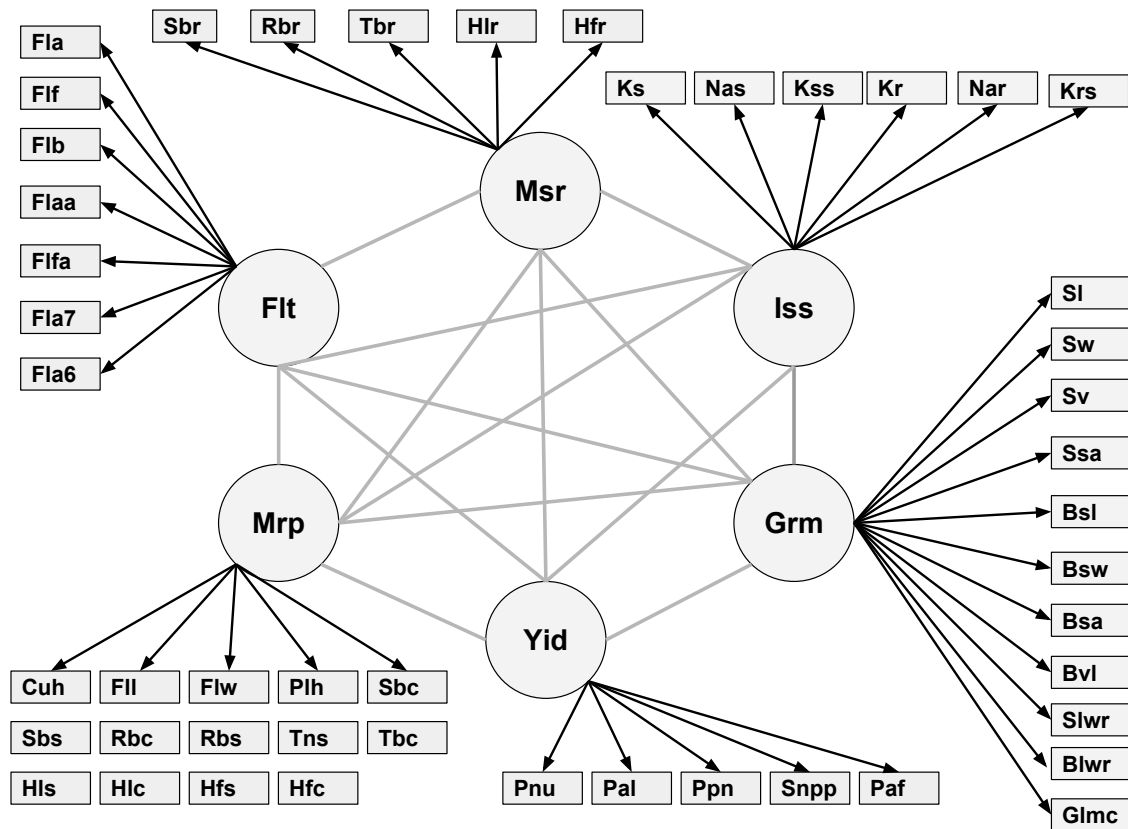| Latent variable	Observed phenotype	Loading
Flowering time	Flowering time at Arkansas (Fla)	0.990
Flowering time	Flowering time at Faridpur (Flf)	0.500
Flowering time	Flowering time at Aberdeen (Flb)	0.578
Flowering time	FT ratio of Arkansas/Aberdeen (Flaa)	-0.212
Flowering time	FT ratio of Faridpur/Aberdeen (Flfa)	-0.549
Flowering time	Year07 Flowering time at Arkansas (Fla7)	0.926
Flowering time	Year06 Flowering time at Arkansas (Fla6)	0.886
Morphology	Culm habit (Cuh)	0.227
Morphology	Flag leaf length (Fll)	0.116
Morphology	Flag leaf width (Flw)	-0.044
Morphology	Plant height (Plh)	0.440
Morphology	Shoot BM Control (Sbc)	0.534
Morphology	Shoot BM Salt (Sbs)	0.456
Morphology	Root BM Control (Rbc)	0.418
Morphology	Root BM Salt (Rbs)	0.280
Morphology	Tiller No Salt (Tns)	-0.349
Morphology	Tiller No Control (Tbc)	-0.318
Morphology	Ht Lig Salt (Hls)	0.920
Morphology	Ht Lig Control (Hlc)	0.899
Morphology	Ht FE Salt (Hfs)	0.907
Morphology	Ht FE Control (Hfc)	0.925
Yield	Panicle number per plant (Pnu)	0.190
Yield	Panicle length (Pal)	0.455
Yield	Primary panicle branch number (Ppn)	0.790
Yield	Seed number per panicle (Snpp)	0.780
Yield	Panicle fertility (Paf)	-0.085
Grain Morphology	Seed length (Sl)	0.251
Grain Morphology	Seed width (Sw)	0.876
Grain Morphology	Seed volume (Sv)	0.990
Grain Morphology	Seed surface area (Ssa)	0.901
Grain Morphology	Brown rice seed length (Bsl)	0.158
Grain Morphology	Brown rice seed width (Bsw)	0.837
Grain Morphology	Brown rice surface area (Bsa)	0.902
Grain Morphology	Brown rice volume (Bvl)	0.986
Grain Morphology	Seed length/width ratio (Slwr)	-0.476
Grain Morphology	Brown rice length/width ratio (Blwr)	-0.432
Grain Morphology	Grain length McCouch2016 (Glmc)	0.047
Ionic components of salt stress	Na K Shoot (Ks)	0.983
Ionic components of salt stress	Na Shoot (Nas)	0.975
Ionic components of salt stress	K Shoot Salt (Kss)	-0.265
Ionic components of salt stress	Na K Root (Kr)	0.061
Ionic components of salt stress	Na Root (Nar)	0.000
Ionic components of salt stress	K Root Salt (Krs)	-0.095
Morphological salt response	Shoot BM Ratio (Sbr)	0.410
Morphological salt response	Root BM Ratio (Rbr)	0.395
Morphological salt response	Tiller No Ratio (Tbr)	-0.022
Morphological salt response	Ht Lig Ratio (Hlr)	0.665
Morphological salt response	Ht FE Ratio (Hfr)	0.939

Figures

Figure 1: Relationship between six latent variables and observed phenotypes. Msr: morphological salt response; Iss: ionic components of salt stress; Grm: grain morphology; Yid: yield; Mrp: morphology; Flt: flowering time. Abbreviations of observed phenotypes are shown in Table S1.
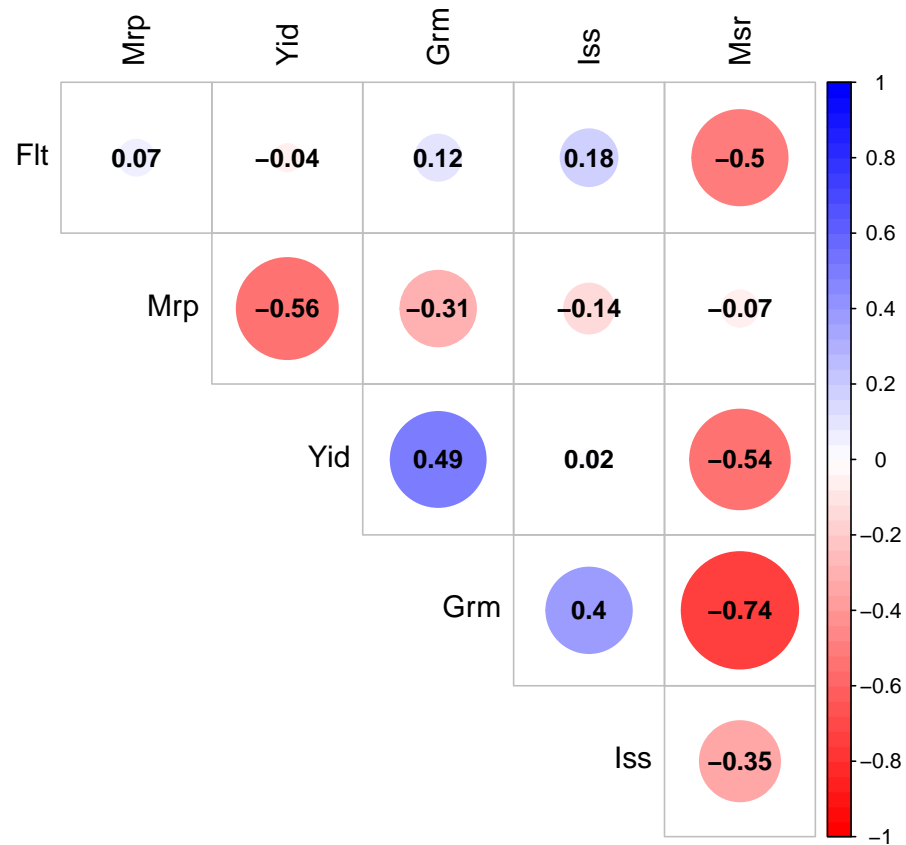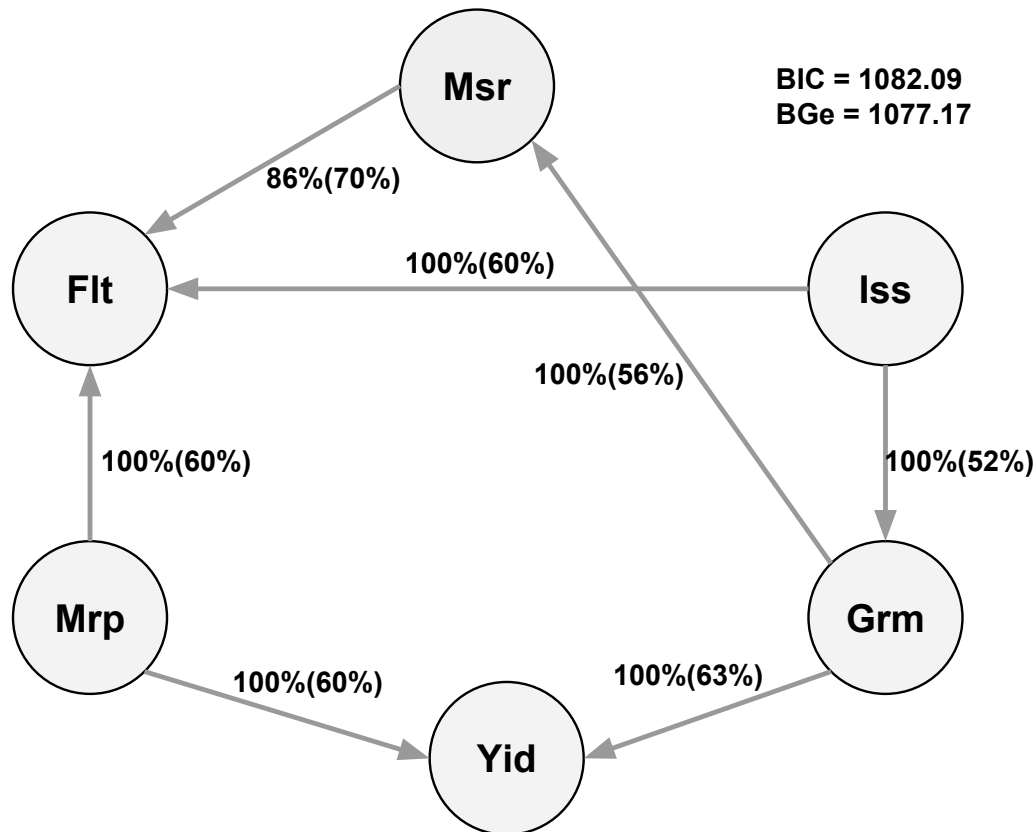
Figure 2: Genomic correlation of six latent variables. The size of each circle, degree of shading, and value reported correspond to the correlation between each pair of latent variables. Msr: morphological salt response; Iss: ionic components of salt stress; Grm: grain morphology; Yid: yield; Mrp: morphology; Flt: flowering time.

Figure 3: Bayesian network between six latent variables based on the Hill Climbing algorithm. The quality of the structure was evaluated by bootstrap resampling and model averaging across 500 replications. Labels of the edges refer to the strength and direction (parenthesis) which measure the confidence of the directed edge. The strength indicates the frequency of the edge is present and the direction measures the frequency of the direction conditioned on the presence of edge. BIC: Bayesian information criterion score. BGe: Bayesian Gaussian equivalent score. Msr: morphological salt response; Iss: ionic components of salt stress; Grm: grain morphology; Yid: yield; Mrp: morphology; Flt: flowering time.
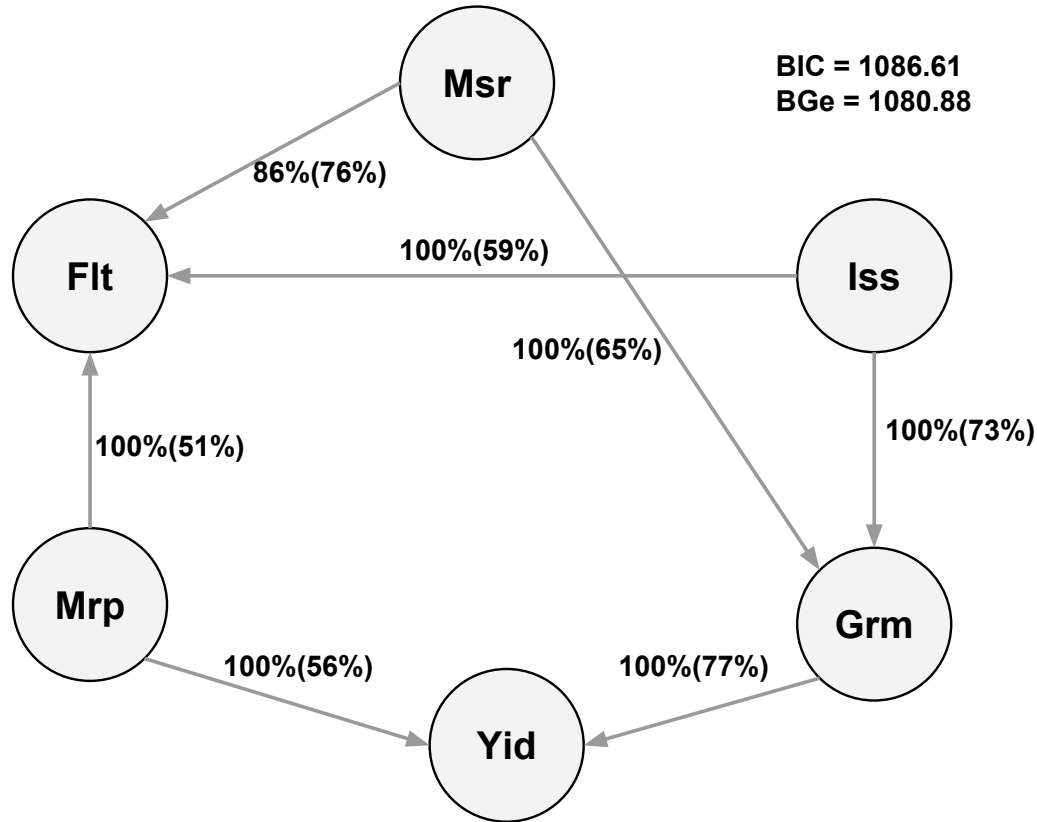
Figure 4: Bayesian network between six latent variables based on the Tabu algorithm. The quality of the structure was evaluated by bootstrap resampling and model averaging across 500 replications. Labels of the edges refer to the strength and direction (parenthesis) which measure the confidence of the directed edge. The strength indicates the frequency of the edge is present and the direction measures the frequency of the direction conditioned on the presence of edge. BIC: Bayesian information criterion score. BGe: Bayesian Gaussian equivalent score. Msr: morphological salt response; Iss: ionic components of salt stress; Grm: grain morphology; Yid: yield; Mrp: morphology; Flt: flowering time.
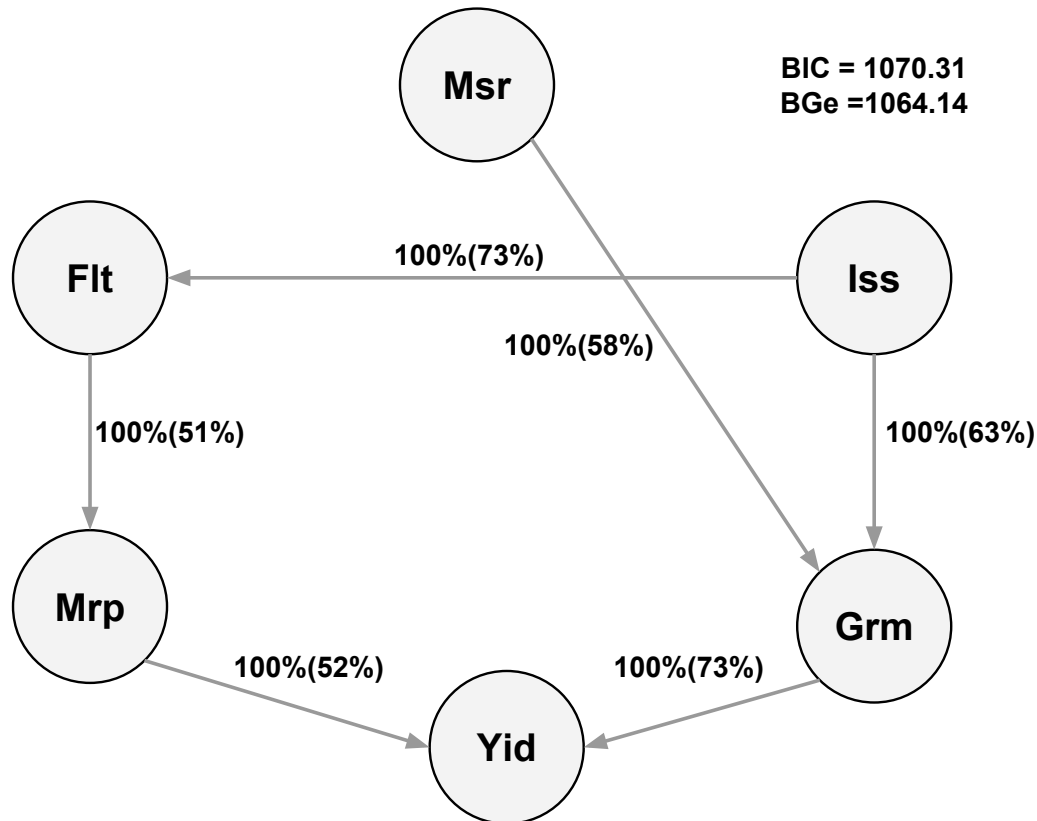
Figure 5: Bayesian network between six latent variables based on the Max-Min Hill Climbing algorithm. The quality of the structure was evaluated by bootstrap resampling and model averaging across 500 replications. Labels of the edges refer to the strength and direction (parenthesis) which measure the confidence of the directed edge. The strength indicates the frequency of the edge is present and the direction measures the frequency of the direction conditioned on the presence of edge. BIC: Bayesian information criterion score. BGe: Bayesian Gaussian equivalent score. Msr: morphological salt response; Iss: ionic components of salt stress; Grm: grain morphology; Yid: yield; Mrp: morphology; Flt: flowering time.
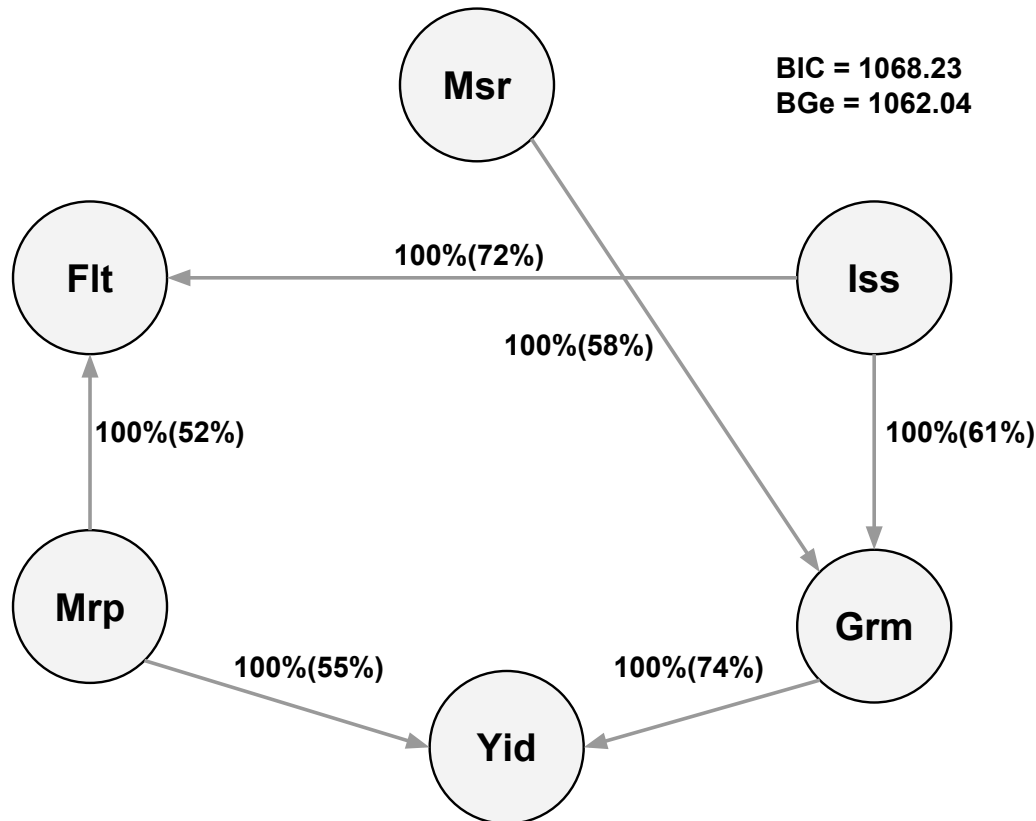
Figure 6: Bayesian network between six latent variables based on the General 2-Phase Restricted Maximization algorithm. The quality of the structure was evaluated by bootstrap resampling and model averaging across 500 replications. Labels of the edges refer to the strength and direction (parenthesis) which measure the confidence of the directed edge. The strength indicates the frequency of the edge is present and the direction measures the frequency of the direction conditioned on the presence of edge. BIC: Bayesian information criterion score. BGe: Bayesian Gaussian equivalent score. Msr: morphological salt response; Iss: ionic components of salt stress; Grm: grain morphology; Yid: yield; Mrp: morphology; Flt: flowering time.